least partly composed of higher altitude particles than their darker surroundings. If this interpretation is correct, then the 500-mbar maps show little sensitivity to the presence of these clouds in the field to the west of the GRS (longitudes to the west of 335°W), either because the upwelling is weak and the 500-mbar temperature difference is too small to measure or because the particles in these clouds are so small as to be ineffective in scattering or absorbing the 22- and 37-μm radiation from which the 500-mbar temperatures are largely derived. However, exceptions to the correlation between visually bright and thermally cool areas abound, including the locally dark STrZ, which is relatively cool, or the visually bright region south of the GRS, a part of which is relatively warm. It is clear that substantial revision will be required of the simple paradigm that regions of upwelling, cold air are associated with saturated gas–producing bright condensate particles.

The GRS temperature field will be further constrained by PPR G1 observations made at high emission angles, which have not yet been completely reduced. Further elucidation of the relationships between the temperature field, circulation, and cloud properties will also be made using maps of nearly all longitudes over a narrow latitude strip just north of the equator (*13*).

REFERENCES AND NOTES

1. E. E. Russell *et al.*, *Space Sci. Rev.* **60**, 531 (1992); Fig. 2 illustrates the bandpasses of the discrete filters compared with a spectrum of Jupiter.
2. J. Spencer, thesis, University of Arizona (1987); M. Urquhart and B. Jakosky, *J. Geophys. Res.* **101**, 21169 (1996).
3. New global controlled mosaic of Voyager Ganymede images prepared by R. Sucharski, (U.S. Geological Survey, Flagstaff, AZ).
4. R. H. Brown and D. L. Matson, *Icarus* **72**, 84 (1987).
5. D. L. Domingue, B. W. Hapke, G. W. Lockwood, D. T. Thompson, *Icarus* **90**, 30 (1991).
6. A. S. McEwen, in preparation.
7. G. J. Veeder, D. L. Matson, T. V. Johnson, D. L. Blaney, J. D. Goguen, *J. Geophys. Res.* **99**, 17095 (1994).
8. The recovery of temperatures uses the weighted-Chahine method [M. T. Chahine, *J. Atmos. Sci.* **27**, 960 (1970)] with additional weighting between the different filters according to their signal-to-noise ratios. The 1σ equivalent δT = 1.3 K for the 15-μm channel, 1.4 K for the 22-μm channel, 0.8 K for the 25-μm channel, and 1.6 K for the 37-μm channel, assuming average atmospheric radiances and averages of four samples for the channels at 15, 22, and 25 μm and 16 samples for the 37-μm channel, corresponding to the observing sequence used for the data reported here. In the radiative transfer model, the He mixing ratio of 13.6% reported by von Zahn and Hunten [*Science* **272**, 849 (1996)] was used, as was a value for the fraction of *para*-H_2 of 0.31 taken from Sada *et al.* (9).
9. P. V. Sada, R. F. Beebe, B. J. Conrath, *Icarus* **119**, 311 (1996).
10. F. M. Flasar, B. J. Conrath, J. A. Pirraglia, *J. Geophys. Res.* **86**, 8759 (1981).
11. G. S. Orton *et al.*, *Science* **265**, 625 (1994).
12. R. Carlson *et al.*, *ibid.* **274**, 385 (1996).
13. Not long after the start of these extensive observations, the PPR filter wheel was found to have remained at the position corresponding to the 37-μm discrete filter, despite commands to move to other filter positions. Therefore all subsequent measurements, including almost all the longitudes of this sequence, were made in the 37-μm discrete filter. Interpretation of these data without independent constraints on cloud properties will be challenging. Our G1 calibration target observations were also made only with this filter, which will make difficult our reexamination of the radiometric calibration.

14. We thank the Galileo Mission Project for their support and carrying this work through. We also thank A. Lacis and J. Hansen for leadership during the early phases of the PPR instrument development, E. Russell for design work, J. Ferrier for maintaining a radiometric calibration scheme, and H. Peiris and C. Connor for their work in processing the data.

4 September 1996; accepted 26 September 1996

Galileo Plasma Wave Observations in the Io Plasma Torus and Near Io

D. A. Gurnett, W. S. Kurth, A. Roux, S. J. Bolton, C. F. Kennel

The Galileo plasma wave instrument detected jovian radio emissions, narrowband upper hybrid waves, and whistler-mode emissions during the inbound pass through the Io torus. The upper hybrid waves provided an accurate profile of electron density through the Io torus and in the vicinity of Io. These measurements show that the torus density has increased by about a factor of 2 since the Voyager 1 flyby in 1979. A well-defined peak in the electron density was observed in the wake of Io, with densities as high as about 4×10^4 per cubic centimeter.

Here we give an overview of results from the Galileo plasma wave instrument during the inbound pass through the Io torus on 7 December 1995, including the flyby of Io. The plasma wave subsystem (PWS) was designed to measure the spectrum of plasma waves and radio emissions over a frequency range from 5 Hz to 5.6 MHz (*1*). During the inbound pass, magnetospheric particle and fields data were obtained from 15:21 to 18:25 UT (universal time). This period includes the Io closest approach (CA) at 17:46 UT. Intense jovian radio emissions called hectometric radiation (*2, 3*) are evident in the electric field spectrogram at frequencies above 1 MHz (Fig. 1). At somewhat lower frequencies, an intense narrowband emission line extends across the electric field spectrogram at frequencies of a few hundred kilohertz. Narrowband emissions of this type are observed in the magnetospheres of Earth (*4*) and the outer planets (*2, 5*) and are caused by electrostatic waves at the upper hybrid frequency f_{UH}. At even lower frequencies, an intense band of noise extends across both the electric-field and the magnetic-field spectrograms in the frequency range from a few hertz to a few kilohertz (Fig. 1). The presence of a magnetic component in this frequency range, between the proton cyclotron frequency (~10 to 30 Hz) and the electron cyclotron frequency (~20 to 60 kHz), uniquely identifies this noise as whistler-mode emissions (*6*). The same type of noise was detected during the Voyager 1 pass through the Io torus (*7*); however, Voyager did not have a magnetic antenna, so a unique mode identification was not possible. Whistler-mode emissions of this type are believed to be generated by energetic radiation-belt electrons (*8*).

Considerable variability exists in the intensity of the whistler-mode noise (Fig. 1). Numerous steplike enhancements lasting several minutes can be seen, for example, from 17:09 to 17:15 UT. Comparisons with data from the energetic-particle detector (EPD) show that these enhancements are closely correlated with increases in the intensity of trapped 15- to 300-keV electrons (*9*). Large variations in the spectrum and intensity of the low-frequency electric and magnetic noise can also be seen near the point of closest approach to Io. A brief, intense burst of broadband electric and magnetic field noise in the downstream wake of Io, from about 17:45:30 to 17:47:30 UT, corresponds almost exactly with the region where the EPD instrument detected an intense bidirectional field-aligned beam of 15- to 100-keV electrons (*10*), apparently accelerated in the vicinity of Io.

The emission line at f_{UH} provides an accurate method of determining the local electron density. The upper hybrid frequency is given by $f_{UH} = (f_p^2 + f_c^2)^{1/2}$

D. A. Gurnett and W. S. Kurth, Department of Physics and Astronomy, University of Iowa, Iowa City, IA 52242, USA.
A. Roux, Centre d'Etudes des Environnements Terrestre et Planetaires, Universite Versailles Saint Quentin, 10/12 Avenue de l'Europe, 78140 Velizy, France.
S. J. Bolton, Jet Propulsion Laboratory, 4800 Oak Grove Drive, Pasadena, CA 91109, USA.
C. F. Kennel, Office of the Chancellor, University of California, Los Angeles, CA 90095, USA.

where f_p is the electron plasma frequency and f_c is the electron cyclotron frequency (6). The electron plasma frequency is given in hertz by $f_p = 8980\sqrt{N}$, where N is the electron number density in particles per cubic centimeter, and the electron cyclotron frequency is given in hertz by $f_c = 28B$, where B is the magnetic field strength in nanoteslas. The electron density can be computed from f_{UH} and f_c using the equation $N = (f_{UH}^2 - f_c^2)/(8980)^2$ cm^{-3}. In the Io torus it is usually the case that $f_{UH} \gg f_c$, so under these conditions it is adequate to use a simple magnetic field model for f_c. We used the O_4 model of Acuna and Ness (11).

The calculated electron density in the torus gradually increased from about 7×10^2 cm^{-3} at 7.5 R_J (jovian radii) to about 4×10^3 cm^{-3} at 5.9 R_J, just before the Io flyby (Fig. 2). As Galileo flew through the wake of Io, the electron density increased sharply, reaching a peak of about 4.1×10^4 cm^{-3} at 17:46:43 UT (12). A broad secondary peak of about 5.3×10^3 cm^{-3} occurred a few minutes after the Io flyby, at about 17:50:27 UT. Thereafter, the electron density declined rapidly, reaching a nearly constant plateau of about 4.5×10^2 cm^{-3} after about 18:10 UT. Except in the vicinity of Io, the electron densities are believed to be accurate to within about ±5%. Near Io, rapid time variations and other complexities lead to larger uncertainties (12).

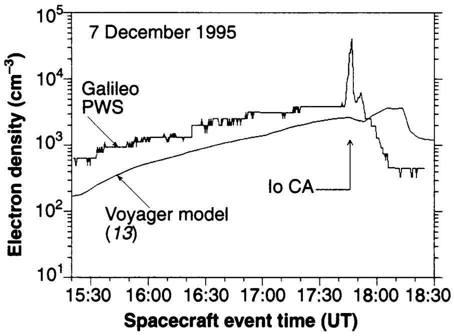

Fig. 2. The electron density profile obtained from the upper hybrid emission line. Also shown is the profile based on Voyager 1 measurements (13). CA, closest approach to Io.

The electron density along the Galileo trajectory has been computed by Bagenal (13), using an empirical model of the torus based on Voyager 1 measurements (14). Beyond the orbit of Io, the Galileo electron densities are consistently about a factor of 2 larger than the Voyager measurements (Fig. 2). This increase suggests that volcanoes on Io, which are the source of the torus plasma, may now be more active than they were during the Voyager era. Inside the orbit of Io, the two profiles are quite different. Most likely these differences are the result of longitudinal effects. Voyager 1 and Galileo passed through the torus at different System III longitudes. Substantial longitudinal effects are known to be present inside the orbit of Io (15).

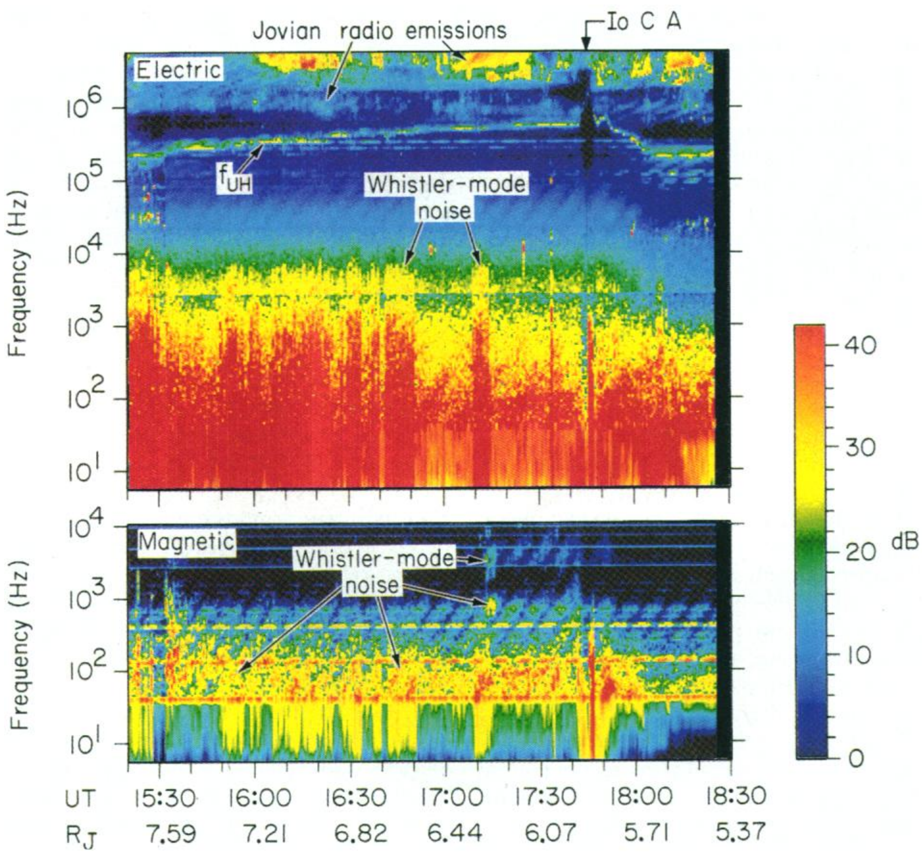

Fig. 1. Frequency-time spectrograms of the electric and magnetic field intensities obtained from the Galileo PWS during the inbound pass through the Io torus on 7 December 1995. The intensities are color-coded, with blue representing the lowest intensities and red representing the highest intensities. Universal time (UT) is in hours and minutes and the radial distance from Jupiter is in jovian radii (1 R_J = 71,492 km). The various horizontal lines, particularly in the magnetic field spectrogram, are spacecraft-generated interference.

REFERENCES AND NOTES

1. D. A. Gurnett *et al.*, *Space Sci. Rev.* **60**, 341 (1992).
2. J. W. Warwick *et al.*, *Science* **204**, 995 (1979).
3. J. W. Warwick *et al.*, *ibid.* **206**, 991 (1979); H. P. Ladreiter and Y. Leblanc, *Astron. Astrophys.* **226**, 297 (1989); M. J. Reiner, J. Fainberg, R. G. Stone, *J. Geophys. Res.* **98**, 18767 (1993).
4. D. Walsh, T. F. Haddock, H. F. Schulte, *Space Res.* **4**, 935 (1964); S. R. Mosier, M. L. Kaiser, L. W. Brown, *J. Geophys. Res.* **78**, 1683 (1973).
5. W. S. Kurth *et al.*, *Geophys. Res. Lett.* **7**, 57 (1980); T. J. Birmingham *et al.*, *J. Geophys. Res.* **86**, 8497 (1981); D. A. Gurnett, *Science* **212**, 235 (1981); D. A. Gurnett, W. S. Kurth, F. L. Scarf, R. L. Poynter, *ibid.* **233**, 106 (1986); D. A. Gurnett *et al.*, *ibid.* **246**, 1494 (1989).
6. T. H. Stix, *The Theory of Plasma Waves* (McGraw-Hill, New York, 1962), p. 12.
7. F. L. Scarf, D. A. Gurnett, W. S. Kurth, *Science* **204**, 991 (1979).
8. J. A. Van Allen *et al.*, *ibid.* **188**, 459 (1975); C. E. McIlwain and R. W. Fillius, *J. Geophys. Res.* **80**, 1341 (1975); F. L. Scarf and N. L. Sanders, *ibid.* **81**, 1787 (1976); F. L. Scarf *et al.*, *Geophys. Res. Lett.* **6**, 653 (1979); R. T. Thorne and B. T. Tsurutani, *ibid.*, p. 649; and others.
9. D. J. Williams, personal communication.
10. D. J. Williams *et al.*, *Science* **274**, 401 (1996).
11. M. H. Acuna and N. F. Ness, *Jupiter* (Univ. of Arizona Press, Tucson, 1976), p. 830.
12. Because the upper hybrid line is not continuous through the wake of Io, some of the electron densities have been computed from the propagation cutoff of jovian radio emissions at f_p. This method is not as reliable as the upper hybrid technique and may overestimate the electron density.
13. F. Bagenal, *J. Geophys. Res.* **99**, 11043 (1994).
14. H. S. Bridge *et al.*, *Science* **204**, 987 (1979).
15. N. M. Schneider and J. T. Trauger, *Astrophys. J.* **450**, 450 (1995).

16. We would like to acknowledge the considerable effort of the Galileo team at the Jet Propulsion Laboratory that was required to make this project a success. Special thanks are also given to L. Granroth and J. Groene for their assistance in the data processing at the University of Iowa. This research was supported by contract 958779 with the Jet Propulsion Laboratory.

6 September 1996; accepted 20 September 1996